GEOPHYSICAL RESEARCH LETTERS, VOL. 27, NO. 19, PAGES 3109-3112, OCTOBER 1, 2000

Seismic anisotropy of the shallow crust at the Juan de Fuca Ridge

Javier Almendros [1,4], Andrew H. Barclay [2], William S. D. Wilcock [3] and G. M. Purdy [2,5]

Abstract. Microearthquake data recorded on four ocean bottom seismometers are used to study shear-wave splitting on the Endeavour Segment of the Juan de Fuca Ridge. The covariance matrix decomposition method is used to determine the sensor orientation from explosive shot data and to estimate the anisotropy parameters for 238 earthquake records. At three of the four sites, the results show a remarkably consistent fast direction parallel to the ridge axis. The time delays between the fast and the slow waves range from 40 to 200 ms, with an average of 90 ms. They are not clearly related to earthquake range, focal depth or source-receiver azimuth. The splitting of the shear waves is interpreted as an effect of structural anisotropy due to the presence of ridge-parallel cracks in the shallow crust. If we assume that anisotropy is concentrated in the upper 1-2 km, the splitting times require a high crack density of ∼0.1.

Introduction

A number of studies have reported observations of seismic anisotropy in the upper oceanic crust [e.g., *White and Whitmarsh*, 1984; *Shearer and Orcutt*, 1985]. This anisotropy is attributed to the preferential ridge-parallel alignment of cracks and fissures, many of which are believed to form near the ridge axis by extensional processes [*Stephen*, 1985]. One of the consequences of seismic anisotropy is shear-wave splitting. The S wave generated by an earthquake source is linearly polarized, but when it goes through an anisotropic region, it splits into two orthogonal components that travel at slightly different velocities. The first portion of the recorded shear wave comprises only the fast wave, and is thus linearly polarized. The polarization becomes nonlinear after the arrival of the slow wave. Measurements of shear-wave splitting can constrain the orientation and density of cracks in the shallow crust [*Crampin*, 1985].

In this paper, we investigate the anisotropy of the young oceanic crust by analyzing the splitting of shear waves recorded during a microearthquake experiment on the Endeavour segment of the Juan de Fuca Ridge (JdFR).

[1]Instituto Andaluz de Geofisica, Univ. de Granada, Spain.
[2]Department of Geology and Geophysics, Woods Hole Oceanographic Institution, Woods Hole, Massachusetts.
[3]School of Oceanography, Univ. of Washington, Seattle.
[4]Now at U.S. Geological Survey, Menlo Park, California.
[5]Now at Division of Ocean Sciences, National Science Foundation, Arlington, Virginia

Paper number 2000GL011535.
0094-8276/00/2000GL011535$05.00

Experiment setting and configuration

The Endeavour segment lies in a tectonically complex region near the northern end of the JdFR (Figure 1). It is offset at either end by overlapping spreading centers and there is extensive seamount volcanism to the northwest. The central portion of the Endeavour is characterized by ridge-parallel bathymetry, similar in appearance to other segments of the JdFR [*Kappel and Normark*, 1987]. An axial high is split by a 100 m-deep, 1 km-wide valley, which is highly fissured, and devoid of recent lava flows. At least four large, high-temperature vent fields are spaced about 2 km apart along the axial valley [*Delaney et al.*, 1992]. Levels of seismicity are much higher on the Endeavour segment than elsewhere on the JdFR [*McClain et al.*, 1993; *Dziak and Fox*, 1995].

In the summer of 1995, a seismic network comprising 15 three-component ocean bottom seismometers (OBS) was

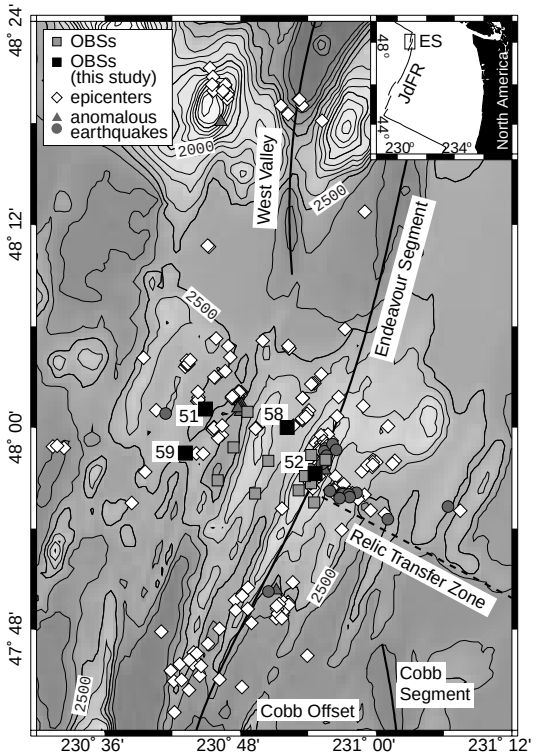

Figure 1. Map of the Endeavour segment showing the OBS network (squares), the four instruments used in this study (black squares) and the epicenters of the earthquakes with clear splitting (open diamonds). Seafloor depths are labeled in meters (contour interval 100 m). Earthquakes for which the fast shear-wave has anomalous directions (see discussion) are shown as gray circles (110°) and triangles (60°).

Table 1. Sensor orientations

OBS	Number of shots	H1 azimuth (°)
51	25	253 ± 8
52	32	36 ± 10
58	48	80 ± 5
59	47	133 ± 4

deployed for 55 days on the central portion of the Endeavour Segment (Figure 1). Seven of the instruments were located in a tight network along a 5 km section of the ridge axis including the Main and High Rise hydrothermal vent fields, with the remainder up to 15 km off axis on the lightly sedimented west flank. Fifty-one explosive charges were detonated within and around the network to determine the instrument locations. High levels of seismicity were recorded in the lower crust both on and off axis, and hypocentral parameters have been determined for nearly 2000 microearthquakes (Wilcock et al., A microearthquake study on the Endeavour Segment of the Juan de Fuca Ridge, in preparation).

Method

We apply the covariance matrix decomposition method (CMDM) [*Jurkevics*, 1988; *Zhang and Schwartz*, 1994] to determine the direction and rectilinearity of the horizontal particle motions. The covariance matrix of the horizontal channels is calculated for a short time window and the eigenvalues and eigenvectors are then obtained. The CMDM provides the rectilinearity, defined as $1 - \lambda_2/\lambda_1$, where λ_1 is the largest eigenvalue and λ_2 the second, and the azimuth of the eigenvector corresponding to λ_1, in the sensor axes reference frame. When the rectilinearity is high, this azimuth represents the direction of the linear particle motion.

OBSs sink freely to the seafloor and so sensor orientations were determined using explosive shot data [*Duennebier et al.*, 1987]. We applied the CMDM to the first 0.1 s of the water wave arrival to estimate the apparent azimuth of the first motion, and converted this to an estimate of the sensor orientation using the known source-receiver azimuth. For each OBS, we averaged the calculated sensor orientations for all shots using the rectilinearity as a weighting factor.

The fast shear-wave direction and the time delay between the fast and the slow waves were also estimated using the CMDM. Since the ray incidence is nearly vertical (6-27°), the azimuth of the particle motion corresponds to the fast direction. Figure 2 illustrates our procedure for an earthquake-OBS pair whose locations are shown in Figure 2a. First, we filter the seismogram with a 15-Hz low-pass Butterworth filter, and select a 1.5-s window centered on the S-wave arrival (Figure 2c). Then, we apply the CMDM to calculate the rectilinearity (Figure 2d) and the azimuth (Figure 2e) of the particle motion, using a 0.0625-s (8-sample) moving window. We select the time interval of high rectilinearity (shown by the vertical dotted lines) that corresponds to the initial S wave motion before the onset of the slow S wave and get the averaged values of rectilinearity and azimuth. Taking into account the sensor orientation, we obtain the azimuth of the fast direction and rotate the horizontal components of the seismogram into the slow and fast directions (Figure 2f). If the waveforms look similar (after reversing one polarity if necessary), the delay time can be estimated from the lag between the matching waveforms (Figure 2g). Figure 2b shows the particle motion for the portion of the seismogram between the dashed lines with the interval of high rectilinearity in bold.

Results

Because of the rough bathymetry in the region, a high proportion of the OBS sensor packages did not deploy level and the data are unsuitable for shear-wave splitting analysis. At least one horizontal channel failed on several other instruments. For these reasons, our study is limited to four OBSs, one on-axis and three on the western flanks (Figure 1). For the four selected OBSs, the sensor orientations determined for individual shots are very consistent and have standard deviations of $\leq 10°$ (Table 1).

Over one thousand records with an S-wave signal-to-noise ratio exceeding $\sim$5 were selected for the splitting analysis. We rejected records if the onset of the S wave was unclear or

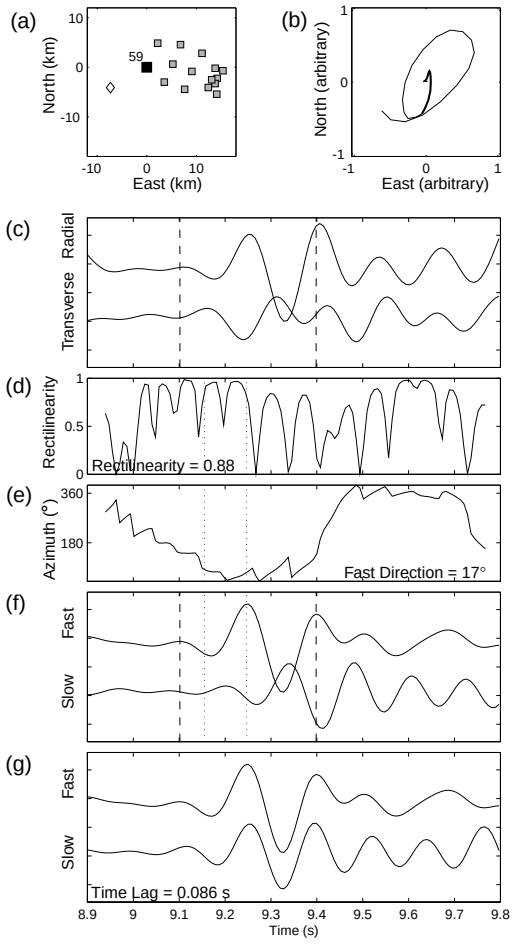

Figure 2. Example of the shear wave splitting analysis. (a) Location of the seismic network (gray squares) and the earthquake (diamond) and OBS (black square) used for this analysis; (b) Particle motion; (c) Original traces; (d) Rectilinearity; (e) Azimuth; (f) Rotated traces; and (g) Matching waveforms. Dashed lines mark the S-wave onset, corresponding to the particle motion plotted in b. Dotted lines show the time interval corresponding to the fast wave arrival (see text for explanations).

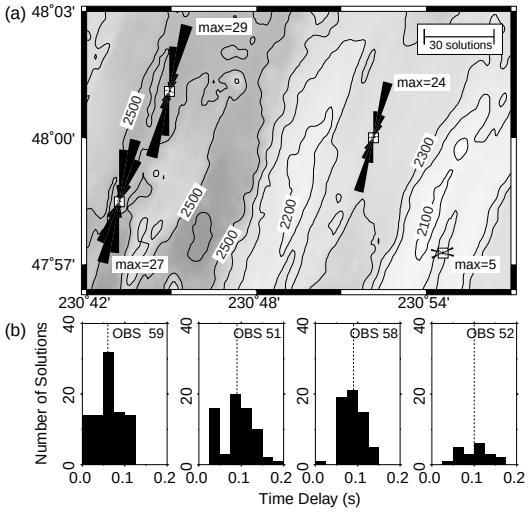

Figure 3. (a) Rose diagrams of the fast direction in 10° bins plotted at the OBS locations. At each site the label max represents the maximum number of solutions within one bin. (b) Histograms of the time delay between the fast and the slow waves. The dotted line shows the average delay.

if the shapes of the rotated waveforms did not match, and were able to determine splitting parameters for a total of 238 records. The earthquakes are located at ranges of up to 40 km and provide fairly good azimuthal coverage. For reasonable oceanic velocity structures, all the angles of incidence are sufficiently steep to fall within the shear-wave window [*Barclay*, 1998] and thus, the S-waves are not contaminated by seafloor phase conversions. The results are summarized in Table 2 and Figure 3. The three off-axis sites have 60-90 solutions each and show a very consistent fast direction at ∼N15°E, which parallels the ridge axis. For the on-axis site, only 20 solutions were obtained and the fast directions are not parallel to the ridge axis; the dominant directions are N60°E and N110°E. The time delay between the fast and the slow S-wave arrival times is heterogeneous at all four sites; it generally falls between 40 and 200 ms with an average of around 90 ms.

Neither the direction of the fast shear wave nor the time delay correlate with the earthquake range, depth or azimuth (Figure 4). A cluster of solutions at back-azimuths of around 120° and with fast directions of about 110° corresponds to earthquakes that lie to the east of the ridge (Figure 1).

Table 2. Splitting parameters

OBS	Measurements	Fast Azimuth (°)	Time Delay (s)
51	68	13 ± 10	0.09 ± 0.04
52	11	58 ± 15	0.08 ± 0.04
	9	110 ± 9	0.12 ± 0.01
58	61	15 ± 11	0.09 ± 0.02
59	86	14 ± 12	0.07 ± 0.03

Discussion

Shear-wave splitting is a consequence of seismic anisotropy and at shallow depths is generally the result of aligned cracks. For vertical cracks, the fast polarization direction coincides with the direction of crack alignment, while the time delay provides information about the crack density [*Crampin*, 1985].

Since the splitting times we measured are independent of earthquake range (Figure 4b), we infer that the anisotropy is concentrated in the shallow crust. Nearly all the earthquakes with well-constrained focal depths are deeper than about 2 km (Wilcock et al., in preparation). Since there is no increase in the splitting time with earthquake depth (Figure 4a), we conclude that the shear wave splitting occurs at depths shallower than 2 km, and is generally localized near the receiver. This inference is supported by the observation that the same earthquake often has different splitting times at different OBSs.

For the three off-axis instruments, we have found a very consistent fast direction and variable time delays. This pattern has been observed in local studies of shear-wave splitting in other environments [*Zhang and Schwartz*, 1994; *Menke et al.*, 1994; *Munson et al.*, 1995]. The orientation of the fast direction is consistent with near-vertical cracks preferentially aligned perpendicular to the spreading direction. The variability in time delays suggests that crack density is heterogeneous. The average time delay of 90 ms requires that the uppermost crust is strongly fractured. By assuming that the upper crust comprises a 500-m-thick layer 2A with S-wave velocities of 1 km/s overlying a region with S-wave velocities increasing uniformly from 2.5 km/s to 3.4 km/s at 2 km depth [*Barclay*, 1998], the split times require an average anisotropy (defined as $2(v_{fast} - v_{slow})/(v_{fast} + v_{slow})$ of 7% in the upper 2 km. Theoretical relationships [*Hudson*, 1981] show that this anisotropy is equivalent to a mean het-

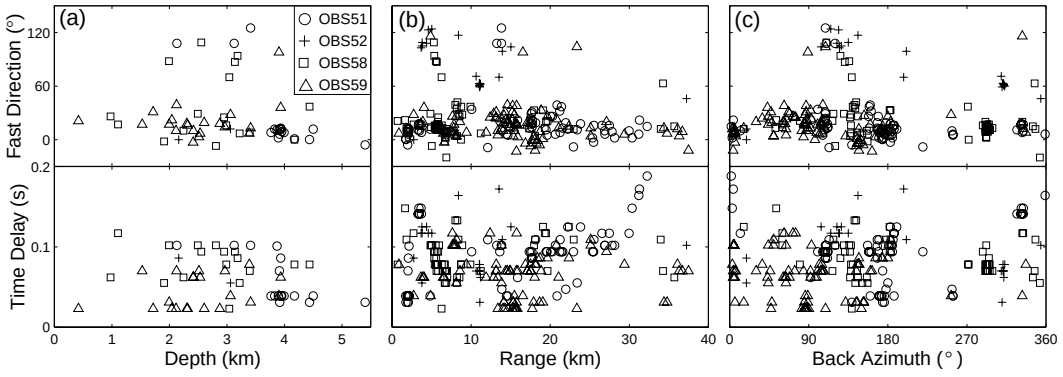

Figure 4. Anisotropy parameters for the four analyzed sites, plotted against earthquake (a) depth, (b) range and (c) back-azimuth. There are fewer points in (a) because the focal depths are unconstrained for events well outside the network.

erogeneous crack density (defined as Na^3/V where N is the number of cracks in volume V and a is the crack radius) of 0.07. If the cracks are concentrated in the upper 1 km, the required anisotropy is 12% and the predicted crack density exceeds 0.1 [*Hudson*, 1981; *Crampin*, 1994].

For the sensor located on-axis, we obtained only a few splitting measurements and the fast directions are not parallel to the ridge axis but are concentrated at azimuths of 60° and 110°. One explanation for the small number of measurements is that signal-to-noise ratios are lower as a result of high levels of attenuation beneath the ridge axis [*White and Clowes*, 1994]. The sensor lies near the Main Endeavour vent field, which has been interpreted as the site of intersecting ridge-parallel and near ridge-perpendicular faults [*Delaney et al.*, 1992]. The fast azimuths at 110° are consistent with the orientation of ridge-perpendicular fractures. The fast azimuths at 60° are qualitatively consistent with a bimodal crack distribution [*Liu et al.*, 1993] with roughly equal crack densities oriented parallel and sub-perpendicular to the ridge. Alternatively, the small number of measurements may simply indicate that there is little anisotropy beneath the axial sensor. The few measurements we have made might be due to near-source splitting or artifacts from effects such as multi-pathing. This explanation is consistent with the hypothesis that the anisotropy of young crust increases as it moves off axis due to the cumulative effects of fissuring and faulting.

There are also a small number of the off-axis measurements that show fast azimuths of 110°. Many of these anomalous azimuths are for earthquakes to the east of the ridge axis (Figure 1). We note that they lie near a relic transfer zone [*Johnson et al.*, 1983] trending ∼110° that previously connected a failed rift on the Cobb segment to the Endeavour segment (Figure 1). Additional measurements of seismic anisotropy will be required to determine whether these anomalous data are influenced by near-source anisotropy.

In summary, the splitting measurements for three off-axis instruments have an average split time of 90 ms and a consistent fast direction of N15°E. These observations can be explained by the presence of ridge-parallel cracks in the upper 2 km of the crust with a crack density of ∼0.1. Our study is generally consistent with previous measurements of crustal anisotropy that indicate high densities of aligned cracks in the shallowmost oceanic crust, both well off-axis [*Shearer and Orcutt*, 1985; *Stephen*, 1985] and on the Mid-Atlantic Ridge [*White and Whitmarsh*, 1984; *Barclay*, 1998].

Acknowledgments. We are grateful to the officers, crew, and scientific party of the R/V Wecoma for assistance in carrying out the experiment. We thank an anonymous reviewer for comments on an earlier draft. This work was supported by the National Science Foundation under grants OCE-9403668 and OCE-9403409. JA also acknowledges partial support by the *Grupo de Investigacion en Geofisica* JA4057 and the grant AP94-24261703 of the Spanish Ministry of Education.

References

Barclay, A. H., Seismicity and structure of the Mid-Atlantic Ridge at 35°N, Ph. D. Thesis, 195 pp., University of Oregon, 1998.

Crampin, S., Evaluation of anisotropy by shear-wave splitting, *Geophysics, 50*, 142-152, 1985.

Crampin, S., The fracture criticality of crustal rocks, *Geophys. J. Int. 118*, 428-438, 1994.

Delaney, J. R., V. Robigou, R. E. McDuff and M. K. Tivey, Geology of a vigorous hydrothermal system on the Endeavour segment, Juan de Fuca Ridge, *J. Geophys. Res., 97*, 19663-19682, 1992.

Duennebier, F. P., P. N. Anderson, and G. J. Fryer, Azimuth determination of and from horizontal ocean bottom seismic sensors, *J. Geophys. Res., 92*, 3567-3572, 1987.

Dziak, R. P., and Fox, C. G., Juan de Fuca Ridge T-wave earthquakes, August 1991 to present: volcanic and tectonic implications (abstract), *Eos Trans. AGU, 76*, F411, 1995.

Kappel, E. S., and W. R. Normark, Morphometric variability within the Axial Zone of the southern Juan de Fuca Ridge: interpretation from SeaMARC II, SeaMARC I and deep-sea photography, *J. Geophys. Res., 92*, 11291-11302, 1987.

Hudson, J. A., 1981, Wave speeds and attenuation of elastic waves in material containing cracks, *Geophys. J. R. Astr. Soc.*, *Geophys. J. Int. 64*, 133-150, 1981.

Johnson, H. P., J. L. Karsten, J. R. Delaney, E. E. Davis, R. G. Currie and R. L. Chase, A detailed study of the Cobb Offset on the Juan de Fuca Ridge: evolution of the propagating rift, *J. Geophys. Res., 88*, 2297-2315, 1983.

Jurkevics, A., Polarization analysis of three-component array data, *Bull. Seismol. Soc. Am., 78*, 1725-1743, 1988.

Liu, E., S. Crampin, J. H. Queen and W. D. Rizer, Behaviour of shear waves in rocks with two sets of parallel cracks, *Geophys. J. Int. 113*, 509-517, 1993.

McClain, J. S., M. L. Begnaud, M. A. Wright, J. Fondrk, J., and G. K. Von Damm, Seismicity and tremor in a submarine hydrothermal field: the northern Juan de Fuca ridge, *Geophys. Res. Lett., 20*, 1883-1886, 1993.

Menke, W., B. Brandsdottir, S. Jakobsdottir, and R. Stefansson, Seismic anisotropy in the crust at the mid-Atlantic plate boundary in south-west Iceland, *Geophys. J. Int. 119*, 783-790, 1994.

Munson, C. G, C. H. Thurber, Y. Li, and P. G. Okubo, Crustal shear wave anisotropy in southern Hawaii: spatial and temporal analysis, *J. Geophys. Res., 100*, 20367-20377, 1995.

Shearer, P., and J. Orcutt, Anisotropy in the oceanic lithosphere - theory and observations from the Ngendei seismic refraction experiment in the south-west Pacific, *Geophys. J. R. Astr. Soc., 80*, 493-526, 1985.

Stephen, R. A., Seismic anisotropy in the upper oceanic crust, *J. Geophys. Res., 90*, 11383-11396, 1985.

White, D. J. and R. M. Clowes, Seismic attenuation structure beneath the Juan de Fuca Ridge from tomographic inversion of amplitudes, *J. Geophys. Res., 99*, 3043-3056, 1994.

White, R. S., and R. B. Whitmarsh, An investigation of seismic anisotropy due to cracks in the upper oceanic crust at 45°N, Mid-Atlantic Ridge, *Geophys. J. R. Astr. Soc., 79*, 439-467, 1984.

Zhang, Z., and S. Y. Schwartz, Seismic anisotropy in the shallow crust of the Loma Prieta segment of the San Andreas fault system, *J. Geophys. Res., 99*, 9651-9661, 1994.

Javier Almendros, U.S. Geological Survey, 345 Middlefield Road, MS 910, Menlo Park, CA 94025. (e-mail: noba@usgs.gov)

Andrew Barclay, Department of Geology and Geophysics, Woods Hole Oceanographic Institution, Woods Hole, MA 02543. (e-mail: abarclay@whoi.edu)

William Wilcock, School of Oceanography, University of Washington, Box 357940, Seattle, WA 98195-7940. (e-mail:wilcock@ocean.washington.edu)

Michael Purdy, Division of Ocean Sciences, National Science Foundation, 4201 Wilson Boulevard, Arlington, Virginia 22230. (e-mail: mpurdy@nsf.gov)

(Received February 25, 2000; revised May 29, 2000;
accepted July 24, 2000.)